Academic Science Journal

Removal of Methyl Violet Dye Using (Zno/Mwcnts) Nanomaterial

Amir Fahdil Dawood AL-Niaimi[1] and Esraa Ibraheim Mahmood*[2]

[1]Department of Chemistry – College of Science – University of Diyala, Diyala, Iraq
[2]Ministry of Education – General Directorate of Education, Diyala, Muqdadiy

scichems2101@uodiyala.edu.iq

Received: 10 August 2022 **Accepted: 10 October 2022**

DOI: https://doi.org/10.24237/ASJ.01.03.669B

Abstract

The composite (0.8/0.018ZnO/MWCNTs) (w/w) of the nanocomposite was used to remove the methyl violet dye from its aqueous solution. Batch system was used in the adsorption process, and the compounds were diagnosed using (FTIR, XRD, BET, EDX, FE-SEM) techniques. It was found that zinc oxide has a surface area of 27.71 $m^2.g^{-1}$, and the average particle size is 45 nanometers. Z nO/MWCNTs surface area is 38.85 m2.g-1, and the effectiveness of using the compound to remove methyl violet dye from aqueous solution was evaluated using batch adsorption. The amount of dye removal by the adsorbents increases with the increase in contact time. The ideal adsorption was achieved in 40 minutes. The pH of the aqueous solution has an effect on the adsorption process. The largest removal of dye was achieved at pH=7, and the adsorption isotherms were studied using Langmuir isotherm and Freundlich model, where it was found that they are more consistent with the Freundlich isotherm. The kinetics of the reaction were studied using the pseudo-first-order model, and the adsorption process was more consistent with the pseudo-second-order kinetics.

Keywords: ZnO/MWCNTs, Nanoparticles, Adsorption, Methyl Violet dye, Adsorption isotherm, Rate of kinetics

Academic Science Journal

إزالة صبغة الميثيل البنفسجي باستخدام المتراكب النانوي (ZnO / MWCNTs)

عامر فاضل داود[1] واسراء ابراهيم محمود[2]

[1]قسم الكيمياء – كلية العلوم – جامعة ديالى
[2]وزارة التربية والتعليم – المديرية العامة للتربية، ديالى، المقدادية

الخلاصة

تم استخدام المتراكب (ZnO/MWCNTs0.018/0.8) (وزن / وزن) لمركب النانوي للإزالة صبغه المثيل البنفسجي من محلولها المائي تم استخدام نظام الدفعة في عمليه الامتزاز وتم تشخيص المركبات باستخدام التقنيات (FTIR, XRD, BET,EDX,FE-SEM) حيث وجد ان اوكسيد الزنك له مساحة سطحيه تبلغ 27.71 m2.g-1ومتوسط حجم حبيبي يبلغ 45 نانومتر المساحة السطحية للمتراكب (ZnO/MWCNTs) وجدت انها تبلغ (138.85 m2.g). تم تقييم فعاليه استخدام المتراكب لإزالة صبغه المثيل البنفسجي من المحلول المائي باستخدام الامتزاز بنظام الدفعات ،تزداد كمية ازالة الصبغة بواسطة الممتزات مع زياده وقت التلامس وتم تحقيق الامتزاز المثالي في 40 دقيقه ،كان للرقم الهيدروجيني للمحلول المائي تأثير ع عمليه الامتزاز حيث كانت أكبر ازالة للصبغة عند الرقم الهيدروجيني,7= PH وتم دارسه ايزوثيرمات الامتزاز باستخدام نموذج فريندليش ولانكماير حيث وجدت انها اكثر تطابقا مع ايزوثيرم فيرندليش ،واظهرت الدراسات التي أجريت على الدوال الثرموديناميكية ان عمليه الامتزاز كانت باعثه للحرارة وتلقائيه ،و تم دراسة حركيات التفاعل باستخدام نموذج المرتبة الاولى والثانية الكاذبة وكانت عملية الامتزاز اكثر تطابقا مع حركيات المرتبة الثانية الكاذبة.

الكلمات المفتاحية: ZnO / MWCNTs ، الجسيمات النانوية ، الامتزاز ، صبغة الميثيل البنفسجي ، ايزوثيرم الامتزاز ، معدل الخواص الحركية

Introduction

The leather, textile, paper, pharmaceutical, and plastics industries are extensively employ dyeing even at low concentrations; however, remnant dye discharge into water resources certainly have deleterious consequences on pyramid diet and aquatic life [1]. It is undesirable for composite textile plants to release colored effluents into the environment due to the fact that many wastewater dyes and their breakdown products are poisonous and/or mutagenic. An industrially relevant hazardous cationic dye with recognized adverse effects on people is methyl violet (MV). The demand for clean water is growing as a result of the increasing water usage by industrial activity in developing countries like China and India [4]. Reduced quantities of

dissolved oxygen are detrimental to humans, animals, and plants. In the leather, textile, paper, pharmaceutical, and plastics sectors, dyeing is frequently employed. Because of this, the removal of these vibrant effluents from wastewater is a major issue for environmentalists worldwide [5]. For a variety of significant water treatment methods, including excellent results have been obtained comprising numerous methods that need additional maintenance costs, energy, and chemical reagents, adsorption is the simplest, least expensive, most widely used, and most successful method for eliminating various organic and inorganic pollutants from water streams [6]. Lately, food chain and carbon nanotubes (CNTs) were acknowledged as superior adsorbent for dyes from waste water due to their distinctive chemo physical properties [9] because of their distinctive chemical and physical properties. In addition, they have specific surface area with low mass density that is chemically inert with specific surface area, a low mass density, and a physically adsorbable surface that is chemically inert, CNTs also feature a highly porous and hollow structure [10]. These remarkable forms have beneficial efficient adsorption properties; thus, CNTs are successfully used to remove a variety of contaminants from wastewater including heavy metals, volatile organic compounds, and dyes [11, 12]

Material and method

Chemicals

Methyl violet is one of the organic compounds that is mainly used as a dye. It is a cationic dye with a molecular formula composed of triphenyl methane, which is considered as a carcinogen due to the aromatic rings in its composition. It is mainly used as a magenta formula for textiles to impart deep violet colors in paints and inks; in addition, it is also used as a wetting indicator for silica gel 13]. The structural formula of methyl violate is described in figure1. The residual MV concentration was determined using a UV-Vis spectrophotometer (Shimadzu UV Spectrophotometer) at a wavelength of 581 nm. According to Beer –lambert low, the absorbance varied linearly with concentration as shown in the calibration curve in Figure 2. Sodium bicarbonate with were used to) 3O) (NaHCO2).3H3zinc nitrate trihydrate (ZnO(NOserve as starting point for creating ZnO nanoparticles.

Academic Science Journal

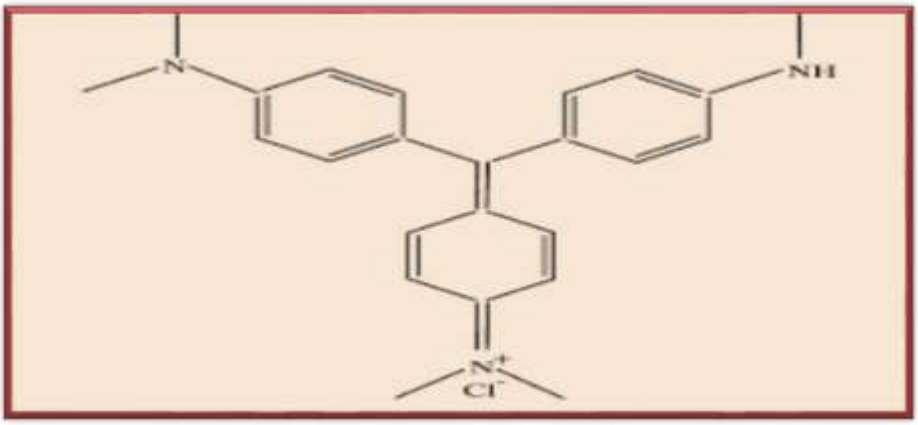

Figure 1: Methyl violet

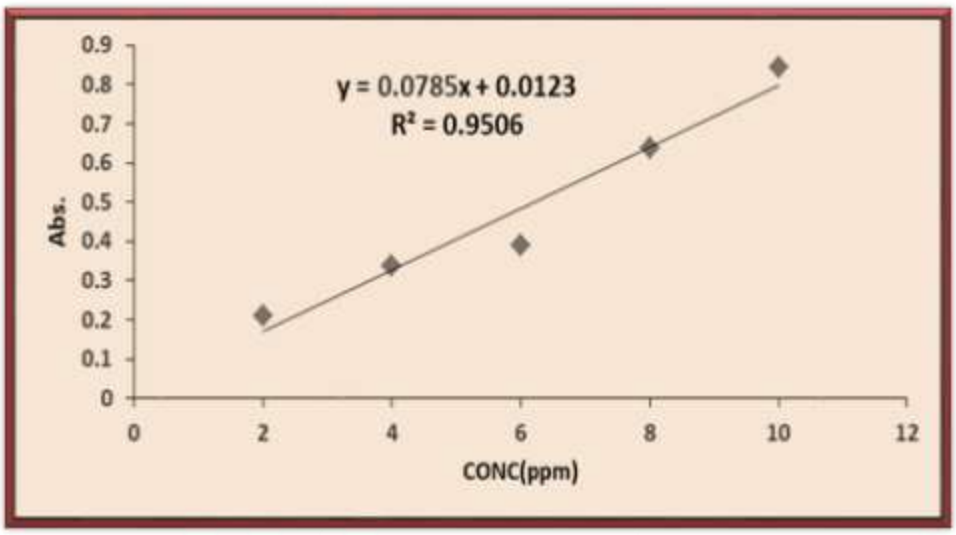

Figure 2: Calibration curve of methyl violet

Preparation of zinc oxide nanoparticle

Zinc oxide nanoparticle was manufactured using a simple precipitation technique using (0.2M) zinc nitrate tri hydrate with the addition of (0.4M) (NaHCO3) in 100 ml of distilled water followed by stirring for 30 minutes to produce homogeneous, transparent solutions. The zinc nitrate aqueous solution was gradually added to the aqueous solution of sodium bicarbonate with continuous mixing at 50 °C until the pH of the mixture reached 6.8, then a white precipitate of particles were generated as a result of this process. The precipitate was filtered and rinsed

with distilled water to remove any residual bicarbonate, then allowed to dry for 2 hours at 80 °C [14].

Preparation of (ZnO/MWCNTs) nanocomposite

To make the (ZnO/MWCNTs) nanocomposite, ethanol solution was used to load the nano zinc oxide (0.8 gm), which was then coated onto the MWCNTs (0.018 g). Before the mixing process, hydrogen peroxide and ammonia were used to "turn on" the multi-walled carbon nanotubes.

Characterizations

As shown in Figure (3), Miller's coefficients was found to be the greatest for the diffraction angles (31.2_34.8_36.4), while studying Zinc oxide nanopartical using X-rays., which match the data on the card with the number (2551-070-01). The figure below displays the precise sectional form of the manufactured nanopartical zinc oxide, the great purity of the crystal growth—no overlapping funnels are visible—and the size of the produced nanopartical grains, which measure 45 nm [14].

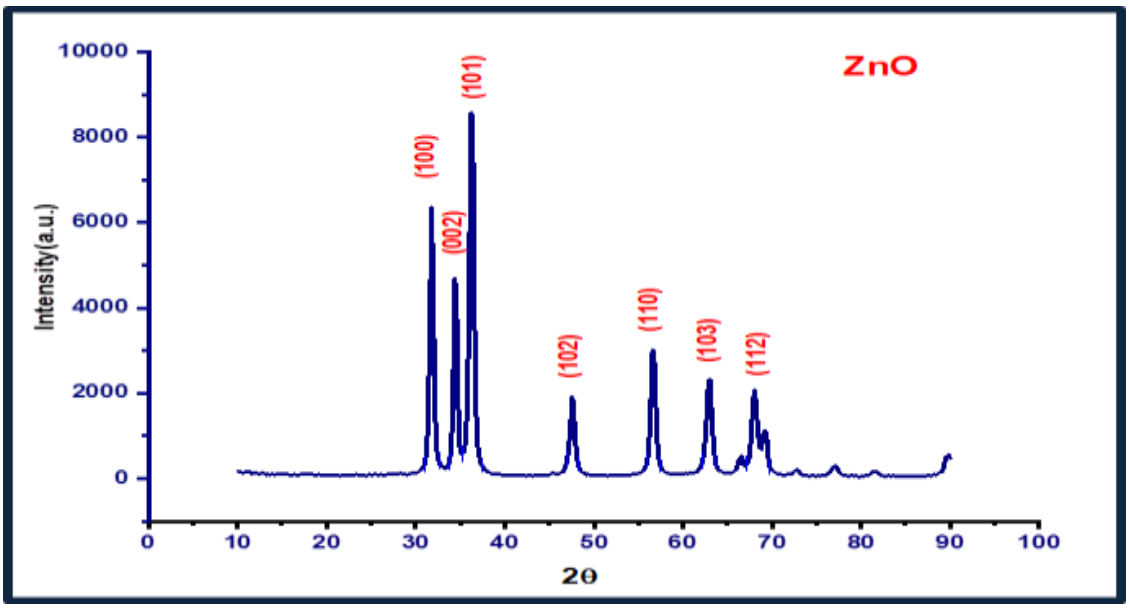

Figure 3: XRD pattern of the prepared (ZnO)

Academic Science Journal

X-ray diffraction of ZNO/MWCNT

The XRD pattern of ZnO nanoparticle-loaded MWCNTS which is shown in figure 4 help to understand the composite's structure (MWCNTs/ZnO). A consequence of Miller's modulus (002) of the peak (26.4), (MWCNTs). The additional peaks of the compound's major characteristic are hexagonal ZnO, according to [15] and [16] JCPDS cards, respectively (card number 79-0205). The XRD pattern showed that ZnO had a pure phase and that there were no parts of the compound that had any further impurities. The strong peaks demonstrated that the sample's zinc oxide was crystallized successfully [17]. Based on the Debbai Scherer equation, it was calculated that the ZnO/MWCNT nanopartical composite is around 13 nm in size.

$$\boldsymbol{D\ crystallite\ size} = \frac{k\lambda}{cos\theta\ ß} \quad \text{..... (1)}$$

Where, D is the crystallite size, λ is the wavelength of the X-ray employed Cu Kα radiation (0.154 nm), β is the Full Width at Half Maximum (FWHM) of the peaks, and θ is the Bragg angle obtained from 2θ value

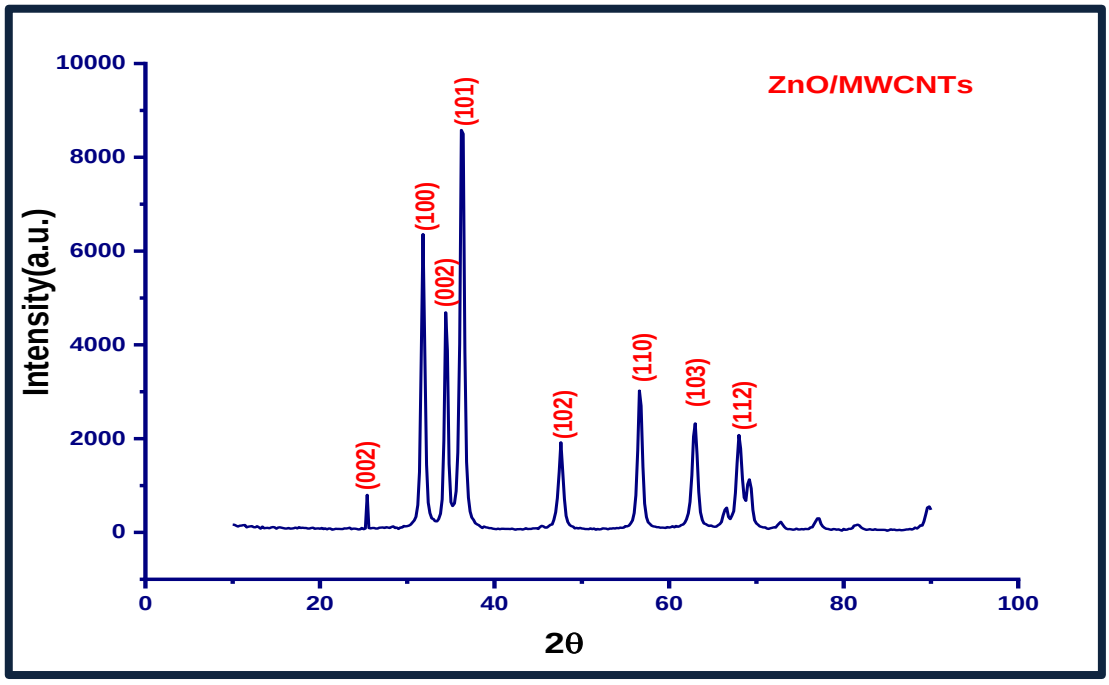

Figure 4: XRD pattern of the prepared (ZnO/ MWCNT)

Academic Science Journal

Analysis of nanomaterials' using an FE-SEM and EDX

Figure (5-a) indicates that ZnO nanopartical layers are present on the surface of (MWCNTs), and Figure (5-b) highlights that the structure resembles a a network-like [18]. The implanted ZnO nanoparticles form bonds with the surface's functional groups; moreover, EDX, which identifies the components in the sample, was used to investigate the characteristics of ZnO NPs and ZnO/MWCNTs [19]. like in Fig (6). The findings demonstrate the presence of Zn.O.C. in the sample as well as the creation of ZnO/MWCNTs. The zinc oxide substance, which has the highest percentage, is shown in the two images (a and b). Despite this, the photo clearly shows the presence of carbon nanotubes (b) despite the small amount that was utilized to create the composite. And (19.91.29.58 nm) is the smallest diameter that was measured.

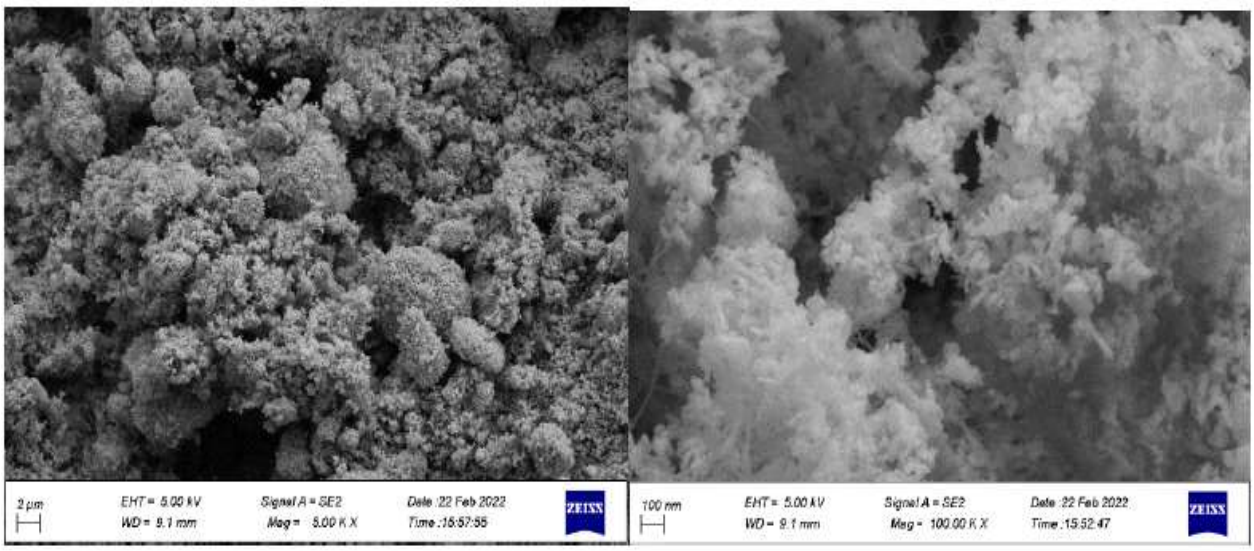

Figure 5: (a,b)FE-SEM of (ZnO/MWCNTs)

Academic Science Journal

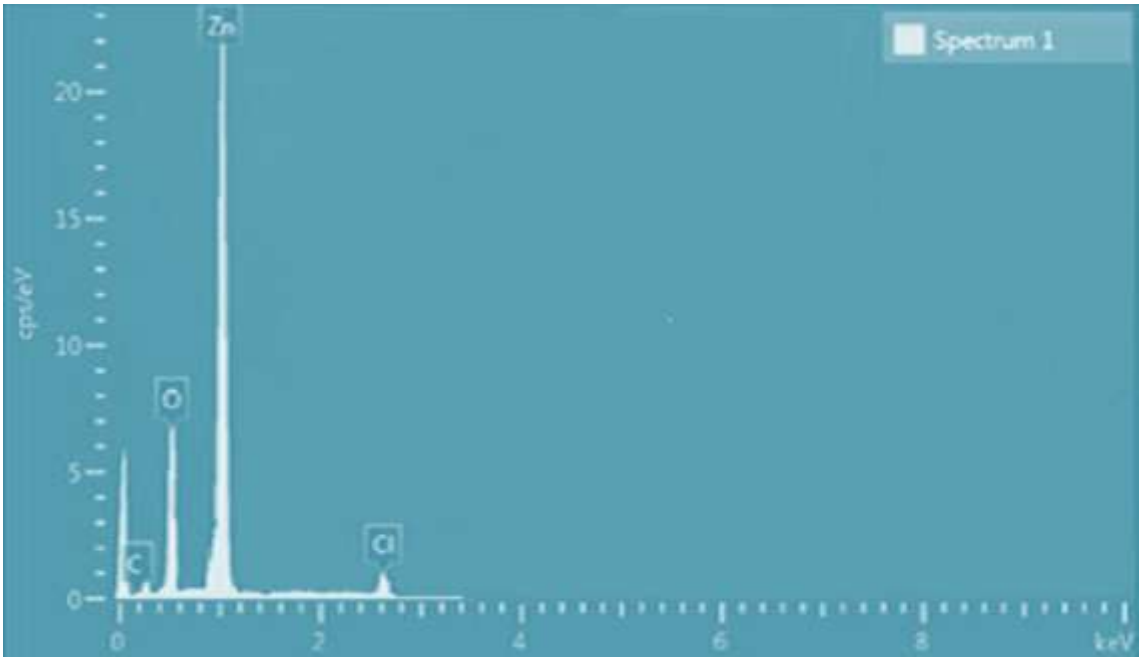

Figure 6: EDX of ZnO/ MWCNT

Figure (7a) depicts the infrared spectrum, which is caused by nano-zinc oxide. The existence of the stretch hydroxyl group, which is a component of the water molecule, may be identified by the absorption band that occurs at a wave number of 3470.82 cm^{-1}, while the apparent absorption bands at wave number (1494.36 cm^{-1}) denote the presence of a (C-C) group, the absorption bands at wave number (1127.14 cm^{-1}) denote the presence of a (C-O) group, and the Zn-O absorption bands at (709.95) cm-1 and (549.11) cm 1 are present in the fingerprint region below (1000) cm 1[20]. The spectrum in Figure (7b), which is the result of (ZnO/MWCNTs), shows fundamental bands of the zinc oxide cause absorption bands at (1.2916.5) cm^{-1}, (3470.82) cm^{-1}, and (417.2) cm^{-1}, respectively [21]. A higher frequency absorption band, cn1(3518.2) cm-1, associated with the hydroxyl group bound to zinc oxide (ZnO), and a second band at (3470.82) cm^{-1}, are seen for the two components of the complex, respectively. Absorption peaks at 1528.6 cm^{-1} and 1135.4 cm^{-1} are attributed to the carbon nanotubes' (C=C) and (C-H) groups, respectively.

Academic Science Journal

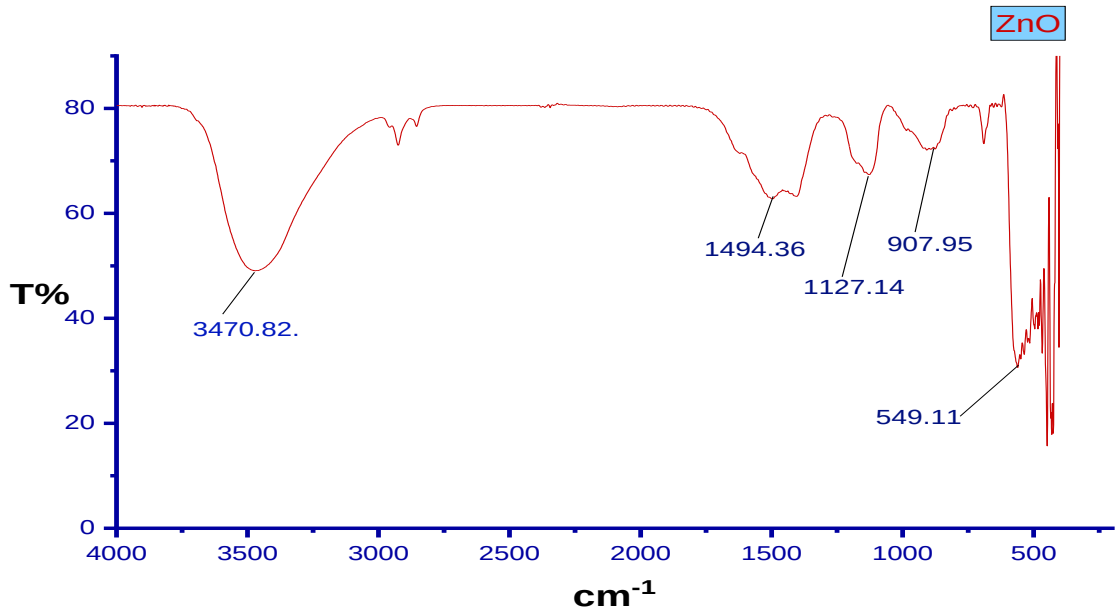

Figure 7: a) Fourier Transform Infrared Spectroscopy of ZnO

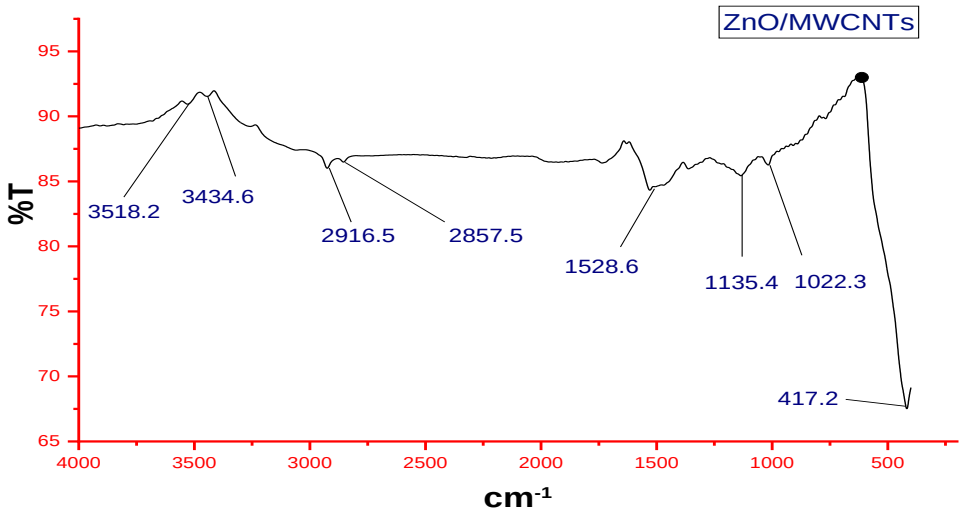

Figure 7: b) XRD pattern of (ZnO /MWCNTs)

Adsorption results

Effect of time

Figure 8 illustrates that the highest clearance rate is at 40 minutes, after which the rate gradually begins to fall. The high starting solution concentration and completely empty active sites on the adsorbent surface resulted in a rapid sorption rate due the solute molecules in the solid and bulk phases interact,[22]

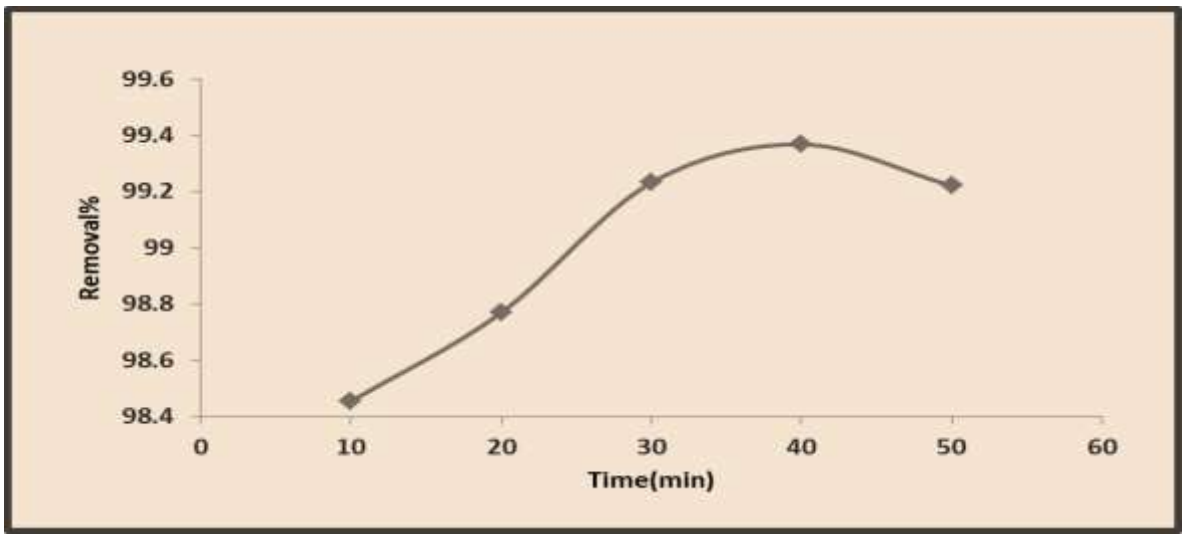

Figure 8: Effect of time of MV adsorption

Effect of (initial concentration)

The initial concentration provides a sufficient driving force to overcome all of the mass transfer barrier between the aqueous and solid phases, as seen in figure 9. For these studies, the initial methyl violet concentrations varied from 10 to 50 ppm and the best concentration to remove the dye was at 10 ppm [23]

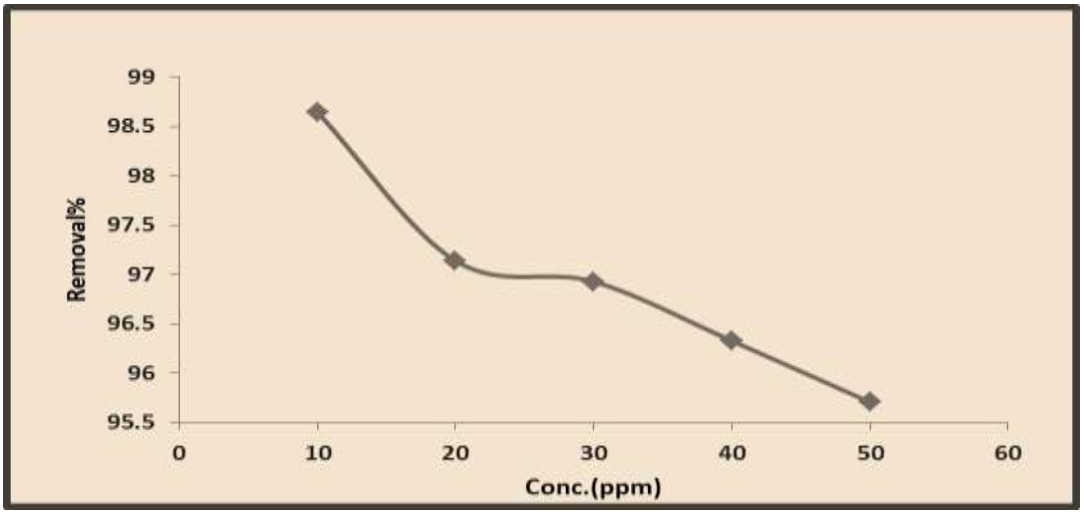

Figure 9: Effect Concentration of MV adsorption

Effect of PH

Since the experiment was conducted the right weight and time for the dyeBy varying the acid function throughout the PH range of 3-11, we were able to examine how this factored into the adsorption process of MV dye on the surface of the composite (ZnO/MWCNTs). It has been shown that the maximum amount of colour may be washed away. at (Ph=7), Adsorption of MV dye and the surface of the aforementioned chemical are shown to be affected by the acidic function in Figure 10 [24].

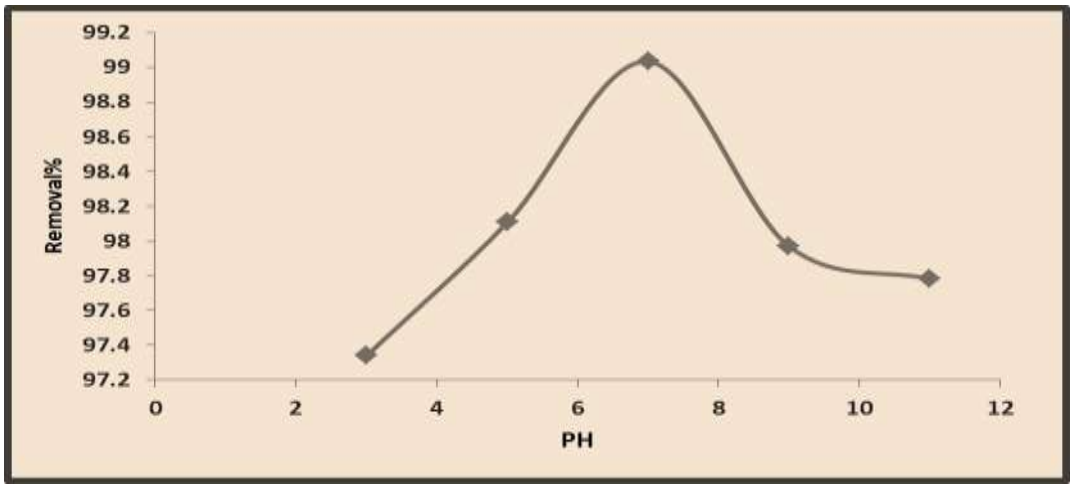

Figure 10: Effect of pH

Academic Science Journal

Kinetic adsorption

Figure 11 shows how the rate of absorption on the adsorbent is determined by adsorption kinetics, and how this affects the adsorption equilibrium time (a,b). Understanding adsorption kinetics is necessary to model the adsorption process, methyl violet adsorption experiment results were Pseudo-first-order and pseudo-second-order adsorption kinetic models were used to analyse the results. Adsorption, as seen in the figure below, is compatible with both pseudo-first-order and pseudo-second-order kinetics, but leans more toward the second-order. .

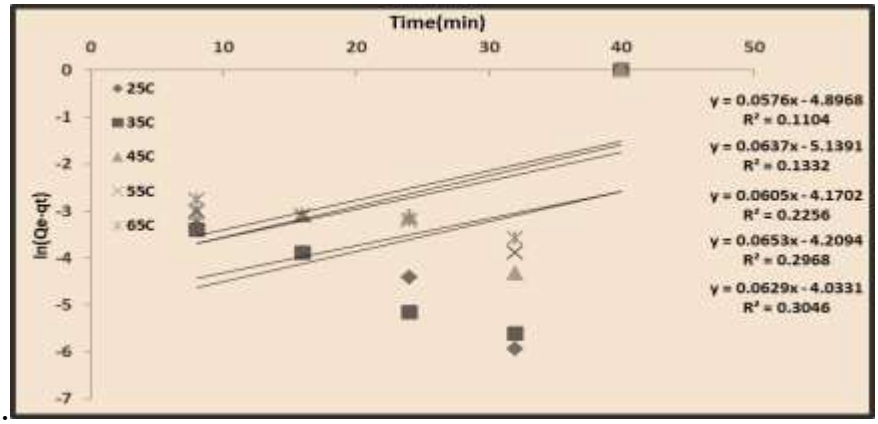

a) pesudo-first-order

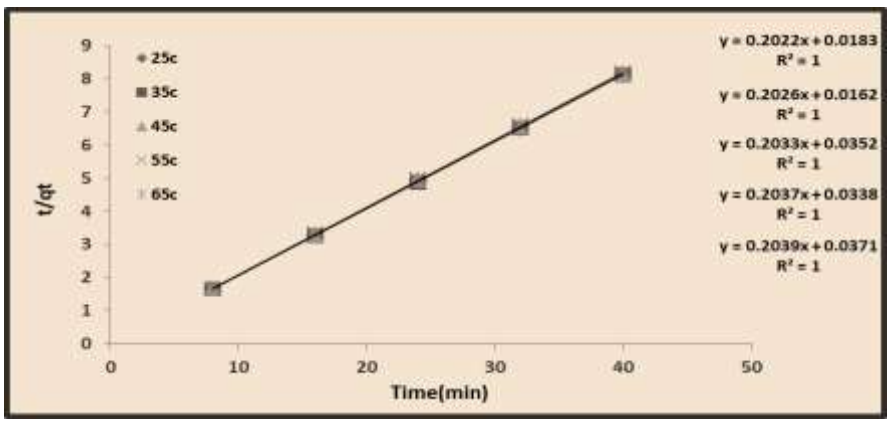

b) pseudo-second-order

Figure 10: (a-b) adsorption kinetic model first and second order

Tablet 1: Adsorption kinetic parameters model first and second order

C0	TC	Pseudo -First-order			Pseudo -Second-order		
		K1 (min^{-1})	qe calc	R^2	K2 ($g.mg^{-1}.min$)	qe calc	R^2
10ppm	25	0.057	0.007	0.11	2.266	4.950	1
	35	0.063	0.005	0.133	2.550	4.950	1
	45	0.06	0.015	0.225	1.177	4.926	1
	55	0.065	0.014	0.296	1.248	4.926	1
	65	0.062	0.017	0.304	1.113	4.926	1

Adsorption isotherm

In certain cases, the term "adsorption isotherm" refers to the connection between, the emphasis of the adsorbent in the solid phase and the concentration of the adsorbate in solution (liquid phase) at a constant temperature. [25]. The equilibrium adsorption, data were analyzed using the Langmuir and Freundlich adsorption isotherm models, respectively. It was fitted using Freundlich equations with the greatest correlation coefficients to describe the isotherms.

Langmuir

This result demonstrates that all adsorption sites on the adsorbent are homogeneous, and the adsorption process is monolayer. A linear equation is used to represent it [26].

$$Ce/Qe = 1/kLQmax + Ce/Qmax \quad \text{..... (2)}$$

Maximum adsorption efficiency (Q max) is expressed in milligrams per gram of material adsorbed, and the dependency constant (KL) ($L.mg^{-1}$). C_e /Q_e vs. C_e linear plots are used to determine the maximum adsorption efficiency and Langmuir constant, respectively. For full monolayer coverage ($mg.g^{-1}$), this procedure produces a straight line with a slope of $1/Q_{max}$ and an intercept of 1/kLQmax.

Freundlich

For the study of removal of a solute from a solution, typically under less-than-ideal conditions, it is one of the most crucial isotherms. According to this theory, substances adsorb on heterogeneous surfaces (Hetro-surfaces), and the locations that the adsorbing surface holds as

adsorption sites vary in attraction from one another. This type of adsorption isotherm is multi-layered rather than single-layered due to the different adsorption sites' varying energy levels, and the Freundlich linear connection is mathematically described as follows [27].

$$\mathbf{lnqe = lnKF + \frac{1}{n} lnCe} \quad \text{..... (3)}$$

KF and n are constants that represent adsorption capacity and intensity, respectively.

Tablet 2: Isotherms parameter

	Langmuir				Freundlich		
T_C	R^2	KL	Q_{max}	RL	R^2	n	KF
25	0.388	0.641	78.740	0.134	0.908	1.123	36.452
35	0.984	0.512	60.975	0.163	0.999	1.270	20.594
45	0.722	0.465	52.910	0.176	0.986	1.383	16.151
55	0.769	0.274	67.567	0.267	0.994	1.248	13.929
65	0.29	0.125	106.383	0.443	0.976	1.157	11.681

Thermodynamic study

The thermodynamic parameter, enthalpy (ΔH) was calculated using the following equation.

$$K_C = A\boldsymbol{e^{-\Delta H / RT}} \quad \text{..... (4)}$$

$$\ln Xm = -\Delta H/RT + K \quad \text{..... (5)}$$

K is the constant in the Van't Hoff equation, R is the universal gas constant (8.314.103 $kJ^{-1}mol^{-1}K^{-1}$), and T is the, temperature. The maximum quantity adsorbed (in mg/g) (Kelvin) is expressed as the natural logarithm, LnXm for example, using [28, 29], G° may be calculated using the Gibs equation: [30].

$$\Delta G° = -RT \ln Kc \quad \text{..... (6)}$$

and **ΔS°** can be fined by, equation

$$\Delta G° = \Delta H - T\Delta S° \quad \text{..... (7)}$$

$\Delta S° = \frac{\mathbf{\Delta H - \Delta G°}}{\mathbf{T}}$ ..... (8)

Thermodynamic functions can be calculated by constant Freundlich [31].

$\boldsymbol{Kc = K_F \rho (\frac{10^6}{\rho})^{(1-1/n)}}$ ..... (9)

K_F = constant Freundlich (mg /g) / (mg /L)

p =water density per unit g/mL 1.0

And to convert constant Freundlich into a unit of equilibrium without units, we follow the following equation [32].

$K_c = K_F * 10^3$ ..... (10)

$\Delta G° = -RTLn(K_F * 10^3)$ ..... (11)

$ln(K_F * 10^3) = \frac{-\Delta H}{RT} + \frac{\Delta S°}{R}$ ..... (12)

Table 2 shows the methyl violet adsorption thermodynamic characteristics on ZnO/MWCNTs. Physical adsorption and chemisorption can be categorized by enthalpy change. MV adsorption seems to be a physical adsorption process with an enthalpy of -0.507 KJ/mol. Positive entropy fluctuations suggest that adsorbent active sites were fixed during random interference at the solid-liquid interface. Negative or zero Gibbs free energy (ΔG°) values showed the spontaneity and feasibility of adsorption without an induction period [33].

Tablet 3: Thermodynamic parameter

C0	Thermodynamic Function	25 C°	35C°	45C°	55C°	65C°
50ppm	ΔG (KJ/mol)	-50.439	-50.934	-51.987	-53.245	-54.583
	ΔH (KJ/mol)	-0.507				
	ΔS (KJ/mol.k)	0.167	0.163	0.161	0.160	0.159

Conclusion

An encouraging finding came from the examination into the multiwall ZnO-treated carbon nanotube. According to the findings, 0.08 g of ZnO loading eliminated Malachite green. Employing batch adsorption tests, the effectiveness of using (ZnO/MWCNTs) to remove methyl violet dye from aqueous solution was assessed. The adsorption equilibrium data were fitted using Freundlich equations, and the isotherms were described. Pseudo-second order models provided a 0.9 accuracy match for the kinetic data. The physical adsorption method known as MV adsorption appears to have both the potential for spontaneity and practicality.

References

1. V. Singh, A. K. Sharma, D. N. Tripathi, R. Sanghi, Journal of hazardous materials, 161(2-3), 955-966(2009)
2. R. G. Priya Narayanan, S. Suresh, C. Muralidharan, (2015). Resolving the benign and the malign isomers of aryl amines by HPLC.
3. T. Cai, Z. Yang, H. Li, H. Yang, A. Li, R. Cheng, Cellulose, 20(5), 2605-2614(2013)
4. A. Saeed, M. Sharif, M. Iqbal, Journal of hazardous materials, 179(1-3), 564-572(2010)
5. M. Monier, D. A. Abdel-Latif, H. A. Mohammed, International journal of biological macromolecules, 75, 354-363(2015)
6. F. Mashkoor, A. Nasar, Journal of magnetism and magnetic materials, 500, 166408(2020)
7. M. K. Uddin, S. S. Ahmed, M. Naushad, Desalination and Water Treatment, 145, 232-248(2019)
8. A. A. Babaei, S. N. Alavi, M. Akbarifar, K. Ahmadi, A. Ramazanpour Esfahani, B. Kakavandi, Desalination and Water Treatment, 57(56), 27199-27212(2016)
9. V. K. Gupta, R. Kumar, A. Nayak, T. A. Saleh, M. A. Barakat, Advances in colloid and interface science, 193, 24-34(2013)
10. Y. H. Li, J. Ding, Z. Luan, Z. Di, Y. Zhu, C. Xu, B. Wei, Carbon, 41(14), 2787-2792(2003)
11. Ö. Kerkez, Ş. S. Bayazit, Journal of nanoparticle research, 16(6), 1-11(2014)
12. I. Hafaiedh, W. El Euch, P. Clement, A. Abdelghani, E. Llobet, Functionalized carbon nanotubes for the discrimination of volatile organic compounds. In: 2013 Transducers & Eurosensors XXVII: The 17th International Conference on Solid-State Sensors, Actuators and Microsystems (TRANSDUCERS & EUROSENSORS XXVII) (pp. 1099-1102). IEEE(2013, June)

13. G. K. Sarma, S. S. Gupta, K. G. Bhattacharyya, RETRACTED: Adsorption of Crystal violet on raw and acid-treated montmorillonite, K10, in aqueous suspension, (2016)

14. M. Fernandez-Garcia, A. Martinez-Arias, J. C. Hanson, J. A. Rodriguez, Chemical Reviews, 104(9), 4063-4104(2004)

15. M. Morsy, M. Helal, M. El-Okr, M. Ibrahim, Spectrochimica Acta - Part A: Molecular and Biomolecular Spectroscopy, 132, 594–598(2014)

16. L. S. Aravinda, K. K. Nagaraja, H. S. Nagaraja, K. U. Bhat, B. R. Bhat, Electrochimica Acta, 95(2010), 119–124(2013)

17. W. Feng, J. Chen, C. yan. Hou, Applied Nanoscience (Switzerland), 4(1), 15–18(2014)

18. T. A. Saleh, M. A. Gondal, Q. A. Drmosh, Nanotechnology, 21(49), (2010)

19. S. Rafique, S. Bashir, R. Akram, F. B. Kiyani, S. Raza, M. Hussain, S. K. Fatima, BioMed Research International, (2022)

20. T. H. Mubarak, K. H. Hassan, Z. M. A. Abbas, In Advanced Materials Research, 685,119-122(2013)

21. C. Violet, P. Franco, O. Sacco, I. De. Marco, Zinc Oxide Nanoparticles Obtained by Supercritical Antisolvent Precipitation for the Photocatalytic, (2019)

22. K. Tewari, G. Singhal, R. K. Arya, Reviews in Chemical Engineering, 34(3), 427-453(2018)

23. R. Ahmad, A. Mirza, Groundwater for Sustainable Development, 7, 101-108(2018)

24. M. Monier, D. A. Abdel-Latif, H. A. Mohammed, International journal of biological macromolecules, 75, 354-363(2015)

25. K. Song, H. Xu, L. Xu, K. Xie, Y. Yang, Bioresource technology, 232, 254–262(2017)

26. J. Fu, Z. Chen, M. Wang, S. Liu, J. Zhang, J. Zhang, Q. Xu, Chemical Engineering Journal, 259, 53-61(2015)

27. S. Wong, H. H. Tumari, N. Ngadi, N. B. Mohamed, O. Hassan, R. Mat, N. A. Saidina Amin, Journal of Cleaner Production, 206, 394–406(2019)

28. A. Fahdil, D. Al-niaimi, F. H. Muhi, Kinetic and Thermodynamic Study on the Removal of Congo Red from the Aqueous Solution Using Graphene Oxide / Magnesium Oxide Nanocomposite, 1–10(2019)

29. A. D. Al-Niaimi, A. A. Olaiwy, International Journal of Research in Pharmacy and Chemistry, 9(1), 23-32(2019)

30. S. Jaerger, A. Dos Santos, A. N. Fernandes, C. A. P. Almeida, Water, Air, & Soil Pollution, 226(8), 236(2015)

31. S. A. Olawale, C. C. Okafor, Journal of Material Science an Reviews, 6(2), 1–11(2020)

32. H. N.Tran, S. J. You, H. P. Chao, Journal of Environmental Chemical Engineering, 4(3), 2671–2682(2016)

33. E. Errais, J. Duplay, F. Darragi, I. M'Rabet, A. Aubert, F. Huber, G. Morvan, Desalination, 275(1–3), 74–81(2011)